Vision, Modeling, and Visualization (2013)
Michael Bronstein, Jean Favre, and Kai Hormann (Eds.)

A Semi-Automated Method for Subject-Specific Modeling of the Spinal Canal from Computed Tomography Images and Dynamic Radiographs

Md. Abedul Haque[1] and G. Elisabeta Marai[1]

[1]Department of Computer Science, University of Pittsburgh, Pittsburgh, USA

Abstract

Shrinkage of the spinal canal may be due to congenital or degenerative conditions, and it causes many spine-related diseases. We present a semi-automated method to computationally reconstruct spinal canal models from static 3D images and dynamic 2D radiographs of the spine. First, we reconstruct the 3D motion of vertebrae from dynamic radiographs and compute hybrid representations of 3D bone models to facilitate computational modeling. We then use the bone position and orientation and the hybrid representations to computationally reconstruct the mesh structure of the spinal canal across the range of motion. The process requires selecting manually only a few landmark points (approximately 1%-2% of all computed vertices), and thus significantly reduces the amount of manual labor required for reconstructing a detailed geometrical model of the spinal canal. Validation on both a healthy and a fusion patient shows that the generated models can capture subject-specific characteristics of the canals and provide insight into the change of the motion pattern due to the surgery. The automation of the method will allow bioengineers to perform large scale experiments on healthy and injured spine joints and thus gain insight into underlying canal conditions.

Categories and Subject Descriptors (according to ACM CCS): Geometric Modeling, Structure from Motion and Stereo, Applications(Medical), Modeling and Simulation, Medical Image Processing and Visualization

1. Introduction

The spinal canal provides a pathway and protection for the spinal cord—a soft-tissue structure of the spine which acts as the conduction pathway for nerve impulses between the brain and the rest of the body. Shrinkage of the spinal canal due to injuries or degenerative conditions can cause serious neurological problems. For example, many cervical fusion patients develop adjacent segment disease [HCP*99] in which segments adjacent to the surgery require further intervention due to pain. The disease is linked with degenerative conditions in the adjacent segments causing nerve compression and pain.

A subject-specific and non-invasive method for automated modeling of the spinal canal with dynamic motion can provide insight into spine-related disorders. Such a method would enable large scale experiments to obtain a better understanding of healthy spine motion and how the spinal cord is affected by motion. However, due to technological limitations, it is practically impossible to capture 3D dynamic images of the spinal cord soft-tissues during normal, loaded movements.

The most common in-vivo approach for computing subject-specific spinal canal measurements is to manually select landmarks in static 3D medical images [FCRC94, MWVB*09]. This manual process is time-consuming and is generally used to compute one or a few specific measurements of the canal. It is impractical to construct a detailed geometric model of the canal—which would require hundreds of points—using this approach.

We propose a semi-automated method for constructing a 3D, subject-specific geometric model of the spinal canal using computed tomography (CT) medical volumes and reconstructed bone motion information. Because the spinal canal is constrained by the surrounding vertebrae, our key idea is that the surface geometry, position and orientation of bones over time can be used to reconstruct and measure geometric

© The Eurographics Association 2013.

DOI: 10.2312/PE.VMV.VMV13.129-136

delivered by EUROGRAPHICS DIGITAL LIBRARY www.eg.org diglib.eg.org

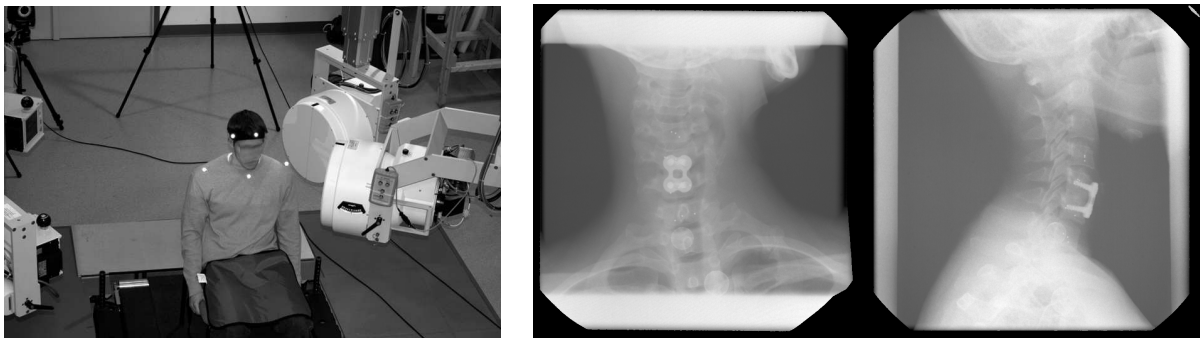

(a) (b)

Figure 1: *A dynamic stereo X-ray (DSX) system (a) was used to capture radiographs during motion. Two X-ray movies are captured from two angles using the system. (b) shows snapshots from the captured X-Ray movies [ABD*11].*

features of the spinal canal. This approach builds on recent advances in motion tracking technology, which enable us to reconstruct accurate bone motion automatically from in-vivo images. The resulting subject-specific geometric models of the spinal canal can help domain practitioners to observe the impact of motion on the spinal canal. These models also help surgeons compare subjects with different conditions, and gain a better understanding of the underlying canal conditions.

2. Related Work

The most common technique for in-vivo analysis is extracting anatomical measurements directly from captured images such as Computed Tomography (CT), Magnetic Resonance (MR) or Radiographs [AA13, MWVB*09, GN85]. Anatomical features are measured from the captured images by manually selecting landmarks in the images. Due to the manual processing steps, the method is time consuming. In addition, geometric details of the spinal canal cannot be obtained in this approach. For example, an in-vivo method based on manually selected landmarks on bone boundaries has been developed to compute the cross-sectional area bounded by the landmark positions [And11]. The method directly uses the manually placed landmark positions to compute the cross-sectional area. Reconstructing 3D geometric models of the spinal canal using this method would require manually placing hundreds of landmarks positions, making the process impractical.

Because the spinal canal deforms significantly during motion, the model needs to be recomputed across the entire range of motion. A geometric model which is constructed by manually selected landmarks and then transformed across the motion, cannot capture the deformation realistically. Therefore, a computational method is essential for accurate modeling and analysis of the spinal canal during motion.

In addition to the in-vivo techniques, accurate spinal canal measurements can be computed directly [PGO*92, CTC*94] through in-vitro experiments on cadaver specimens. Detailed 3D models of the canal can be generated using foam fillings and then digitizing the resulting cast [LTCK09]. However, because of significant subject-specific variations of the spinal canal features, in-vitro experimental measurements cannot be used to build in-vivo subject-specific geometric models.

In conclusion, no semi-automated or automated technique exists for modeling and analyzing spinal canals during motion from in-vivo medical images, that would also provide sufficient geometric detail.

3. Materials and Methods

We present a semi-automated computational method to build subject-specific models of the spinal canal during dynamic motion. The spinal canal contains the spinal cord and the surrounding protective layers. The canal is mainly constrained by the vertebral bodies and two ligament bands (the Posterior Longitudinal Ligament and the Ligament Flavum) along the spinal column.

Because vertebral bodies directly constrain the spinal canal, we use the bone models and their accurate position and orientation information to reconstruct the spinal canal. The dynamic motion information allows us to reconstruct the geometric model of the canal and to capture the changes of the canal during motion.

To generate geometric models of the spinal canal, we first capture 3D volumetric images of bones with a static imaging technique. We then reconstruct the motion information of bones by applying an in-vivo non-invasive model-based method. The method utilizes dynamic 2D X-ray images captured during motion and the bone models generated from the static volumetric images. Next, we compute hybrid representations—meshes and distance-fields—of the

© The Eurographics Association 2013.

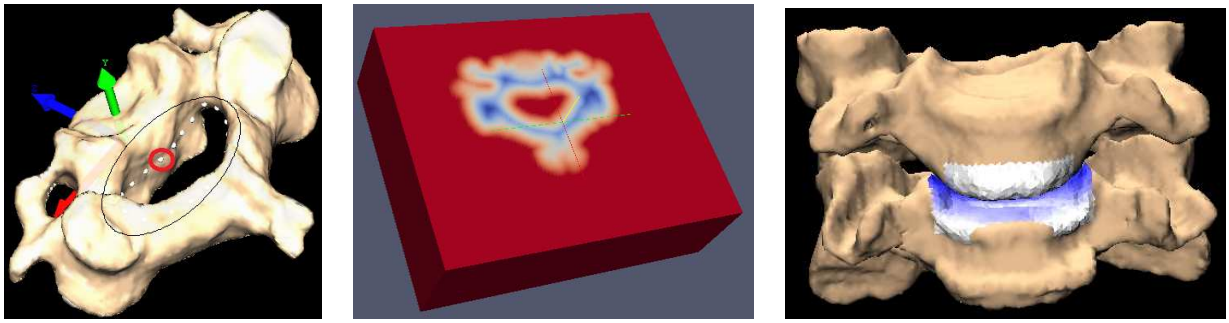

(a) (b) (c)

Figure 2: *(a) The explicit mesh representation of the bone. The spinal foramen region is marked in black and the manually placed landmarks are shown within it. (b) A 2D crosscut through the distance field representation. Red indicates points outside the bone surface and blue indicates points inside the bone surface. The distance from the surface is mapped to the color saturation level. (c) Visualization of the inter-bone joint space computed using the distance-field information; darker colors indicate shorter distance between the two adjacent bone surfaces.*

3D bone geometry; these representations have complementary strengths and facilitate fast computation of inter-bone joint space measurements. We reconstruct spinal canal models during a complete movement sequence using the hybrid representations and motion information of the bones. Finally, we propose geometric features to analyze the spinal canal structure. We describe each step of this pipeline in detail below.

3.1. Data Acquisition and Motion Reconstruction

We use in-vivo conditions and real clinical data for the proposed spinal canal modeling method. We obtain 3D volumetric images of the spine with a high-resolution computed tomography (CT) scanner (Light-Speed 16, GE Medical Systems, Waukesha, WI). We then segment the CT images using 3D medical imaging software (Mimics).

To obtain 3D motion information, we capture high-resolution radiographs (Fig. 1b) with a dynamic stereo X-ray (DSX) system (Fig. 1a). DSX utilizes two frame-synchronized imaging systems each including a 100 kW cardiac cine-radiographic generator, a 0.3/0.6 mm focal spot size X-ray tube, a 40 cm image intensifier and a high-speed camera providing 1800x2400 pixel resolution at up to 500 frames/sec with 14-bit dynamic range.

Next, we reconstruct 3D motion information by applying a highly accurate hierarchical model-based method [HATM13] which has been shown to achieve sub-millimeter accuracy (average precision 0.3mm translation and 1^o rotation) for in-vivo spine data. In this approach, we reconstruct computationally a virtual model of the DSX imaging system and then we simulate X-rays through the bone models to produce a pair of digitally reconstructed radiographs (DRRs). By manipulating the bone models within the virtual DSX system, we can generate pairs of DRRs for any bone position and orientation. Using image similarity—a 85/15 weighted average of cross-correlation and gradient correlation—between the actual radiographic image pairs and the DRRs, we then optimize the position and orientation of each bone to identify the configuration that provides the best match, thus determining the position of the actual bone in the space. The hierarchical model-based method leverages spatial and temporal coherence and the hierarchical overlapping structure of vertebrae to reconstruct the motion automatically and accurately.

3.2. Bone Geometry Representations

To enable computational modeling of the spinal canal, we compute two representations—explicit mesh representation and implicit distance-field representation—of the 3D bone geometry from the CT images of bones. The bone models are segmented with high accuracy by domain experts, and no smoothing or simplification is applied to the models. The resulting geometric models have 10k-20k vertices and 20k-50k faces per vertebra. The explicit mesh representation (Fig. 2a) is used for manual identification of landmarks (approximately 20 per vertebra) and to confirm the correctness of the generated canal models. The implicit distance-field representation (Fig. 2b) enables fast computation of joint-space distances (Fig. 2c) such as the distance between an arbitrary point in the spinal canal and the nearest bone surface.

We compute the vertebrae meshes using the marching cube [LC87] algorithm. To generate distance-field models, we apply a level-set method—the closest point transform [Mau00] to the explicit mesh representation.

© The Eurographics Association 2013.

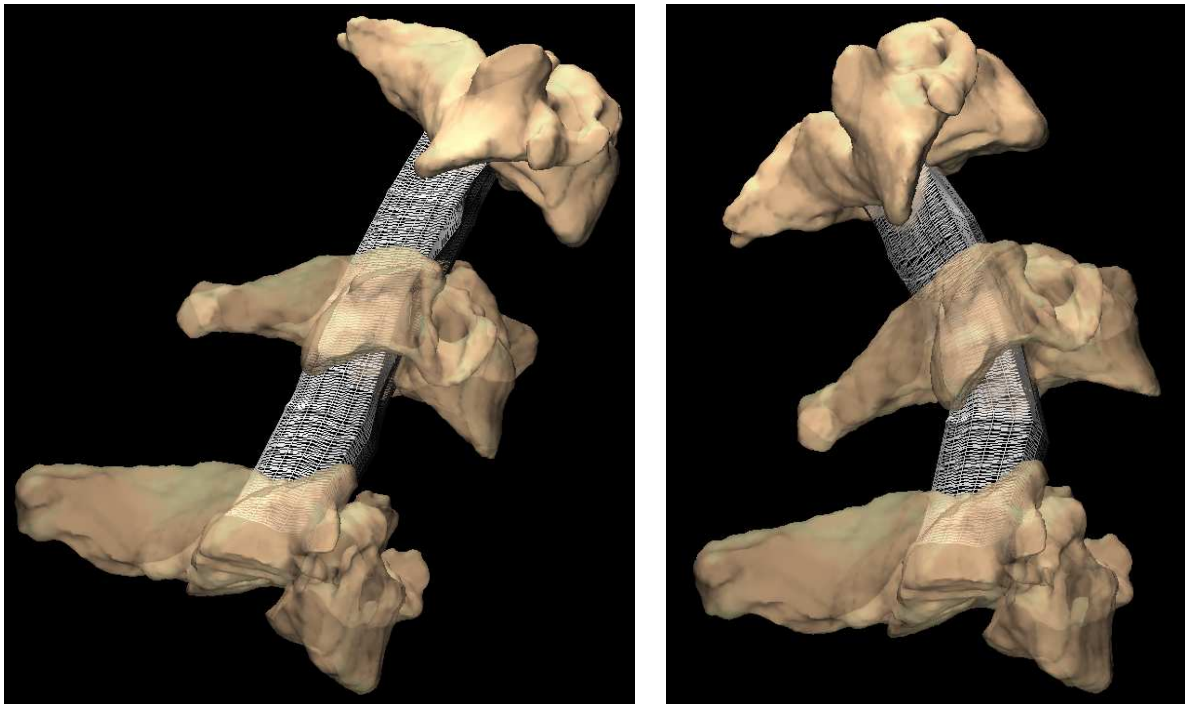

(a) (b)

Figure 3: *The reconstructed spinal canal meshes at two extreme rotations of the neck—full flexion (a) and full extension (b)—during the captured motion sequence. To avoid visual clutter we only show three vertebrae—C3,C5 and C7.*

3.3. Spinal Canal Geometry Reconstruction

From the bone representations and the reconstructed motion information, our method reconstructs the 3D geometry of the spinal canal. Because the spinal canal is constrained by the vertebral foramen (vertebral region which constructs the spinal canal as shown in Fig. 2a), we manually place a few (approximately 20) landmark points, evenly distributed (~ 2 mm apart) around the central circumference of each vertebral foramen (Fig. 2a), starting-from the anterior-side center of the vertebral body (red circle in Fig. 2a). A straight-line visual correspondence is sketched during this step between corresponding landmarks on adjacent vertebrae, to help ensure that the correspondence does not lead to crossings. The spinal canal geometry is then automatically constrained to pass through the landmark points and restricted to not penetrate the vertebral foramen. The total number of points selected manually is a small fraction (approximately 1%-2%) of all computed vertices of the mesh.

To compute the 3D spinal canal geometry, we generate a constrained path between two landmark points of two neighboring vertebrae. First, we identify the starting and the ending landmark points of a path. The constrained path is assumed to be the shortest path between the two landmark points restricted by the bone structures. The constrained path can be thought of as a fiber between the two landmark points. Following [Mar07], we compute the constrained fiber path using an optimization method that exploits the distance field representations of the bones for computational efficiency, as described below.

The optimization algorithm assumes a piecewise linear segment between the two landmark points (p_0 and p_n) of a fiber path. Intermediate points ($p1 \ldots p_{n-1}$) are generated through sampling at uniform intervals. Then the algorithm optimizes the intermediate points to minimize the length of the path through all intermediate points under the constraint that no point is inside any bone model. To ensure efficient computation of the constraints, we use the implicit distance field representation. For any point ($p_{x,y,z}$), the distance-field representation (f) gives the distance (positive if the point is outside the bone surface and negative if the point is inside the bone surface) between the point (p) and the nearest point on the bone surface. The optimization routine minimizes the following cost function

$$\min_{x_i,y_i,z_i} \sum_{i=0}^{n-1} \sqrt{(x_{i+1}-x_i)^2+(y_{i+1}-y_i)^2+(z_{i+1}-z_i)^2} \quad (1)$$

subject to $f(x_i,y_i,z_i) > 0, i = 1 \ldots n-1$.

Since we keep the intermediate points equally spaced

© The Eurographics Association 2013.

along the path, $(x_{i+1} - x_i)$ is constant. Therefore, the optimization problem reduces to

$$\min_{y_i,z_i} \sum_{i=0}^{n-1} \sqrt{const + (y_{i+1} - y_i)^2 + (z_{i+1} - z_i)^2} \qquad (2)$$

subject to $f(x_i, y_i, z_i) > 0, i = 1 \ldots n-1$.

We use a sequential quadratic programming (SQP) method (from the NAG library [NAG]) to solve the optimization problem. However, the optimization method is prone to converging towards local minima. To tackle this challenge, we take advantage of temporal coherence and use the computed geometry of a frame to initialize the optimization process of the neighboring frames. We found that this method converged to the correct solution successfully for all frames of the motion sequences.

To construct the spinal canal model, we first construct multiple interconnected fibers. Individual fiber paths are computed following the approach described above. Then we generate a uniformly distributed equal number of points along all computed fiber paths. We perform a custom triangulation on the points to generate the mesh model of the spinal canal (Fig. 3). Because the canal structure deforms significantly during motion, we generate mesh models for each frame across the motion using the automated method described above.

Because the interior bone surfaces are smooth, the shortest path approximates well the bounding surface: all shortest path approximation points are less than 0.75 mm (averaged over vertebrae and frames) away from the bone surface and a further 85% of these points are less than 0.5 mm from the bone surface.

3.4. Quantitative Analysis

The geometric model of the spinal canal can be used to analyze the effect of motion on the spinal column and the spinal cord. Quantitative analyses on the meshes can be used to extract useful measurements for comparative analysis.

To enable quantitative analysis, we compute the volume of the canal and the volume of each functional segment (i.e. C3-C4, C4-C5, C5-C6 and C6-C7) of the canal. We also compute average deflection or bending of the canal for all frames. Volume and deflection analysis during motion may indicate a potential unhealthy condition of the spinal column. In addition, to quantify the change in spinal canal diameter, we compute a center line through the spinal canal mesh and measure the average distances from the centerline to the mesh surface.

To compensate for subject-specific variation, we compute normalized measurements. We first identify a frame which is the most resembling to the neutral posture. The identification is done manually, since due to subject variability the neutral frame is neither located mid-range of motion nor trivial to detect computationally. To compensate for human error in selecting the reference frame, we take three consecutive frames around the selected frame. We compute volume, radius and deflection for each of these frames, and the mean and standard deviation over this set of frames. We normalize the measurements of the remaining frames (of the motion range) with respect to the measurement of the reference frame. The normalized measurement indicates a change in the spinal canal in percentage rather than in absolute value, and thus enables comparative analysis among subjects.

4. Results

We applied the canal modeling method on real clinical data captured from two subjects. We selected one healthy and one fusion patient to validate that the method allows inter-subject comparison—despite subject-specific geometric variations of the spinal canal—and to test whether the fusion surgical procedure affects the spinal canal deformation during motion. One of the two datasets is a healthy cervical spine (47 years old male); the other dataset is a single level anterior fusion in vertebrae C5-C6 (40 years old female). The fusion patient was tested around 6 months post surgery. We reconstruct the spinal canal segment between vertebrae C3 and C7 so that we can see the impact of the fusion surgery.

We compare the spinal canal models of our subjects in terms of volume, radius, and deflection over the range of motion.

4.1. Volume analysis

Table 1 shows the computed volume of the canal models from the two subjects. Average volume for both reference frames and the full range of motion differs significantly between the two subjects indicating the subject-specific variations of the two models.

Normalized volume analysis for each segment of the spinal column shows an interesting pattern (Table 2): For

Segment	Range of normalized volume change (% of the reference volume)	
	Fusion Subject	Healthy Subject
C3-C4	25%	12%
C4-C5	34%	21%
C5-C6	3%	26%
C6-C7	18%	3%

Table 2: *Normalized volume changes for the spinal canal segments. The subjects show different patterns due to the fusion surgery: The fusion subject has significantly lower volume change in C5-C6 region than the healthy patient. The analysis indicates that in the fusion subject the segments adjacent to C5-C6 are compensating for this difference.*

© The Eurographics Association 2013.

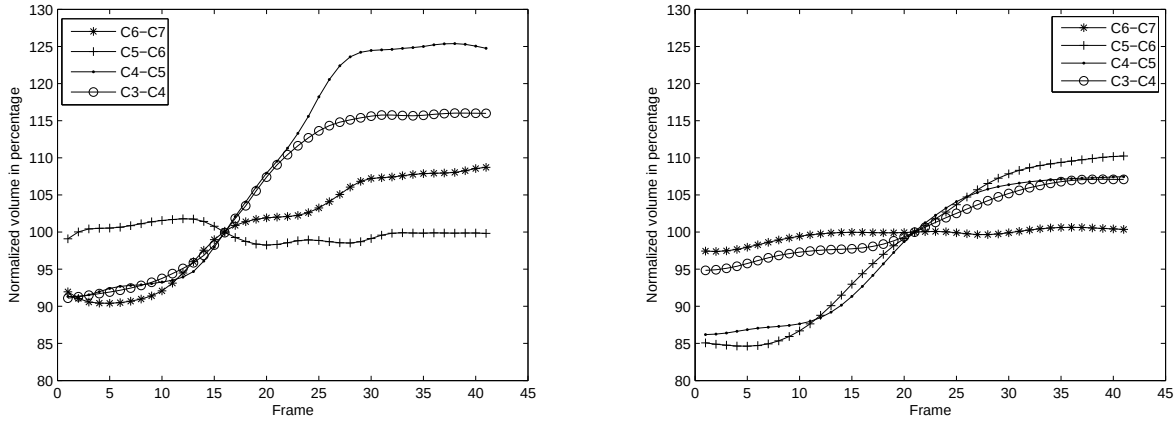

Figure 4: *Normalized volume analyses across the dynamic motion range(from full extension to full flexion) for each segment of the spinal canal for a fusion and a healthy subject. C5-C6 is the least changing volume segment in the fusion patient(a). In contrast, C5-C6 is the most changing segment in the healthy patient (b). Other spinal canal segments of the two subjects are affected differently by the motion.*

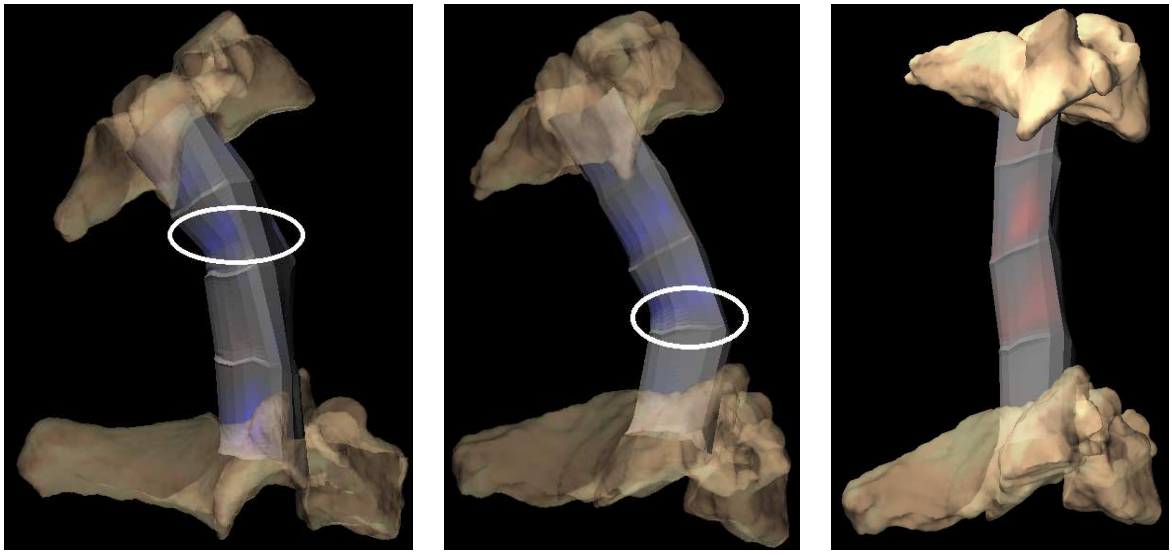

Figure 5: *The difference in the deflection region for the two subjects' spinal canals. For the fusion subject (a), the canal bends towards the top of the spinal column and for the healthy subject (b), the canal bends towards the middle of the spinal column. The change in the spinal canal radius is mapped to the hue (from blue to red; blue for increase and red (c) for decrease in radius) on the canal surface. To avoid visual clutter we only show the vertebrae C3 and C7.*

© The Eurographics Association 2013.

Selected Frames	Mean±Standard Deviation of volume (mm^3)	
	Fusion Subject	Healthy Subject
Volume in the reference frames	14446.57±152.81	16958.7±113.33
Volume over the entire motion range	14999.81±1107.71	16885.5±946.93

Table 1: *Spinal canal volume in the cervical spine (C3-C7) for the healthy and the fusion subject (not normalized). The change in volume is due to subject variation.*

the healthy subject, the C5-C6 segment shows a maximum change in volume during motion (Fig. 4); the change of volume decreases for the surrounding segments C4-C5, C3-C5 and C6-C7. In contrast, for the fusion subject C5-C6 shows the minimum change of volume. This significantly affects the volume change pattern for the other segments. C3-C4, C4-C5 and C6-C7 show significantly different change in volume than the healthy subject.

4.2. Deflection Analysis

We compute the deflection of the spinal canal model across the range of motion. Analysis shows that the deflection of the fusion patient (4.2±0.8mm) is smaller than the deflection of the healthy subject (6.3±1.1mm). More importantly, visualization of the models shows the deflections in the two models are at different locations along the canal (Fig 5). The deflection analysis along with our volume analysis confirms that the effects of motion on the spinal canal of the two subjects are significantly different.

4.3. Spinal Canal Radius Analysis

We analyze the radius of the spinal canal to see whether significant shrinkage can be identified in either of the subjects. In addition, we visualize the narrowing of the canal on the spinal canal surface (Fig 5). We find that the change of radius with respect to the neutral frame is within the range of ±1mm for both subjects. We consider this change insignificant because of the limited resolution of the bone surface models (the CT image resolution is 0.3mm-0.5mm). Our findings agree with the fact that neither of the subjects had symptoms of spinal canal narrowing (spinal stenosis).

4.4. Domain-Expert Feedback

To evaluate the clinical significance of our tool, we presented the tool and the results to a bioengineer and two spine surgeons. The domain-experts stated that the tool could be employed to gain better understanding of spine related conditions such as myelopathy (compression of the spinal cord due to degenerative conditions) and congenital stenosis (compression of the spinal cord due to congenital narrow spinal canal). Spine surgeons generally diagnose these conditions by computing two measurements—the canal diameter, and the ratio between the canal diameter and the vertebral body diameter (Torg ratio [TMM*02]) — from the sagittal plane X-ray or volumetric images of the spine. However, these simple measurements are not always effective to understand the complex dynamic nature of the spinal canal and the underlying conditions. The surgeons remarked that the reconstructed geometric models of the spinal canal will facilitate more detailed analyses and thus help the design of effective and accurate measures to diagnose and understand the conditions. The surgeons are looking forward to applying the tool in a large scale experiment on both healthy and symptomatic spine joints.

5. Discussion and Conclusion

The result analysis shows that the spinal canal geometric models we generate are capable of capturing subject-specific features of the spinal canal. The method is also capable of handling geometric variations of different vertebral bodies and the geometric changes due to fusion. Additionally, comparative analysis between a healthy and a fusion patient shows interesting patterns in the spinal canal volume and deflections; these patterns capture the effect of fusion and the difference between a normal and a fused spinal canal movement. We did not find any significant narrowing of the spinal canal indicating no spinal stenosis for the subjects.

Because we create the spinal canal models semi-automatically from non-invasive in-vivo medical images, the method can be applied in large scale control group studies to gain insight into spinal canal related diseases and injuries. For example, a large scale experiment with spinal stenosis and healthy subjects can lead to insight into spinal stenosis and its effect on the spinal column during motion.

The optimization algorithm we use to find the constrained fiber path is fully automatic and requires approximately 10 minutes per frame in a standard PC (2 GHz processor, 4.00 GB RAM). We pre-compute the geometric models of the spinal canal and then load for real-time visualization and analysis. Parallel computation can significantly reduce the runtime of the optimization method.

The modeling process requires the identification of landmark points and the reference frame. This step requires less than an hour per subject (less than 50 minutes for placing the landmark points on all bones and less than 5 minutes for identifying the neutral frame within the motion sequence). The number of manually selected points is 1%-2% (approximately 20 manually selected points for each mesh segment

© The Eurographics Association 2013.

containing about 1300 computed points) of the total computed points. Thus automation helps us to reduce the human labor significantly (approximately 98% reduction). Please note that the manual step is performed to the best of the user's capability. No in-vivo approach exists today for accurate identification of these features.

In terms of limitations, we did not validate our results against in-vitro data. However, validation of the reconstructed models against in-vitro data would be problematic because the spinal canal deforms significantly when dissected due to the change in loading conditions. Thus, in-vitro validation would lead to inaccurate measurements.

Furthermore, we used a hierarchical model-based motion reconstruction method which has been previously reported to achieve sub-millimeter accuracy for in-vivo cervical spine studies [HATM13]. Using alternative, lower accuracy motion reconstruction methods may affect the quality of the mesh model reconstruction.

In conclusion, we have designed and developed a semi-automatic method to reconstruct the geometric model of the spinal canal from captured images of joints. The method is in-vivo and non-invasive, and it allows subject-specific dynamic analysis of the spinal canal. Due to the automation of the method, we gain approximately a 98% reduction in the number of required landmark points compared to the manual method. The method generates detailed geometrical models and enables comparison between different subjects.

Because the method uses in-vivo data, it can be applied in large scale experiments for validating hypotheses related to spine injuries and diseases. Thanks to its level of automation, the tool has potential for real clinical scenarios and can also be very useful for biodynamics and orthopedic research.

Acknowledgments

We thank Dr. Scott Tashman and Mr. William Anderst (Department of Orthopaedics, University of Pittsburgh, School of Medicine) for the spinal data acquisition and preprocessing, Dr. James Kang, MD, Dr. Joon Y. Lee, MD and Dr. Kevin Bell (University of Pittsburgh Medical Center) for their feedback. This work is supported by grants NSF IIS-0952720 and NIH/NIAMS R03-AR056265. We thank the anonymous reviewers and the Pitt VisLab for their insightful and careful feedback.

References

[AA13] ALY T., AMIN O.: Geometrical dimensions and morphological study of the lumbar spinal canal in the normal egyptian population. *Orthopedics 36*, 2 (Feb. 2013), e229–34. 2

[ABD*11] ANDERST W. J., BAILLARGEON E., DONALDSON W. F., LEE J. Y., KANG J. D.: Validation of a noninvasive technique to precisely measure in vivo three-dimensional cervical spine movement. *Spine Phila Pa 1976 36*, 6 (2011), E393–400. 2

[And11] ANDERST W.: Automated measurement of neural foramen cross-sectional area during in vivo functional movement. *Comput Methods Biomech Biomed Engin* (2011). 2

[CTC*94] CHANG D., TENCER A., CHING R., TREECE B., SENFT D., ANDERSON P.: Geometric changes in the cervical spinal canal during impact. *Spine (Phila Pa 1976) 19*, 8 (1994), 973–80. 2

[FCRC94] FANG D., CHEUNG K., RUAN D., CHAN F.: Computed tomographic osteometry of the asian lumbar spine. *J Spinal Disord 7*, 4 (1994), 307–16. 1

[GN85] GILAD I., NISSAN M.: Sagittal radiographic measurements of the cervical and lumbar vertebrae in normal adults. *Br J Radiol 58*, 695 (1985), 1031–4. 2

[HATM13] HAQUE M., ANDERST W., TASHMAN S., MARAI G. E.: Hierarchical model-based tracking of cervical vertebrae from dynamic biplane radiographs. *Medical Engineering & Physics 35*, 7 (2013), 994–1004. 3, 8

[HCP*99] HILIBRAND A., CARLSON G., PALUMBO M., JONES P., BOHLMAN H.: Radiculopathy and myelopathy at segments adjacent to the site of a previous anterior cervical arthrodesis. *J Bone Joint Surg Am 81*, 4 (1999), 519–28. 1

[LC87] LORENSEN W. E., CLINE H. E.: Marching cubes: A high resolution 3d surface construction algorithm. *Computer 21*, 4 (1987), 163–169. 3

[LTCK09] LI Z., TANG J., CHAKAN M., KAZ R.: Carpal tunnel expansion by palmarly directed forces to the transverse carpal ligament. *Journal of biomechanical Engineering 131*, 8 (2009), 1–18. 2

[Mar07] MARAI G. E.: *Data-Driven Predictive Modeling of Diarthrodial Joints.* PhD thesis, Brown University, 2007. 4

[Mau00] MAUCH S.: A fast algorithm for computing the closest point and distance transform. *SIAM J Sci Comput submitted* (2000), 1–17. 3

[MWVB*09] MALGHEM J., WILLEMS X., VANDE BERG B., ROBERT A., COSNARD G., LECOUVET F.: Comparison of lumbar spinal canal measurements on mri and ct. *J Radiol 90*, 4 (2009), 493–7. 1, 2

[NAG] Nag fortran library routine document, e04ccf. http://www.nag.co.uk/numeric/fl/manual/pdf/E04/e04ccf.pdf. 5

[PGO*92] PANJABI M., GOEL V., OXLAND T., TAKATA K., DURANCEAU J., KRAG M., PRICE M.: Human lumbar vertebrae. quantitative three-dimensional anatomy. *Spine (Phila Pa 1976) 17*, 3 (1992), 299–306. 2

[TMM*02] TIERNEY R., MALDJIAN C., MATTACOLA C., STRAUB S., SITLER M.: Cervical spine stenosis measures in normal subjects. *J Athl Train 37*, 2 (2002), 190–193. 7

© The Eurographics Association 2013.